Taylor & Francis
Taylor & Francis Group

Journal of Coordination Chemistry

ISSN: 0095-8972 (Print) 1029-0389 (Online) Journal homepage: http://www.tandfonline.com/loi/gcoo20

Two Zn(II) coordination polymers based on 1,3-di(4′-carboxyl-phenyl)benzene and N-donor coligands: syntheses, crystal structures, and luminescent properties

Bing Liu

To cite this article: Bing Liu (2015) Two Zn(II) coordination polymers based on 1,3-di(4′-carboxyl-phenyl)benzene and N-donor coligands: syntheses, crystal structures, and luminescent properties, Journal of Coordination Chemistry, 68:7, 1251-1260, DOI: 10.1080/00958972.2015.1019484

To link to this article: http://dx.doi.org/10.1080/00958972.2015.1019484

Journal of Coordination Chemistry, 2015
Vol. 68, No. 7, 1251–1260, http://dx.doi.org/10.1080/00958972.2015.1019484

Two Zn(II) coordination polymers based on 1,3-di(4'-carboxyl-phenyl)benzene and N-donor coligands: syntheses, crystal structures, and luminescent properties

BING LIU*

School of Chemistry and Chemical Engineering, Xinxiang University, Xinxiang, PR China

(*Received 18 August 2014; accepted 30 December 2014*)

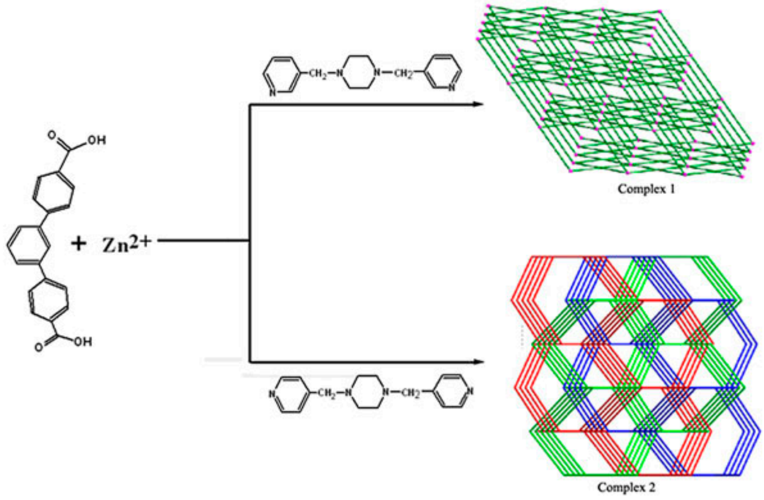

Two coordination polymers, $\{[Zn(dpb)(3\text{-}bpmp)_{0.5}]\cdot 1.5(DMF)\}_n$ (**1**) and $[Zn(dpb)(4\text{-}bpmp)]_n$ (**2**) (H_2dpb = 1,3-di(4′-carboxyl-phenyl)benzene, 3-bpm*p* = 1,4-bis(3-pyridylmethy)piperazine, 4-bpm*p* = 1,4-bis(4-pyridylmethy)piperazine and DMF = N,N-dimethylformamide), were solvothermally synthesized and characterized. Tuning the difference of N-donor ligands, we obtained **1** and **2** which display different topological nets. Complex **1** features a 6-connected topological net and **2** shows a 4-connected three-fold interpenetrated framework. Luminescent properties of **1** and **2** are investigated at room temperature.

Keywords: Zinc(II); Solvothermal; Luminescence; Crystal structure

---

*Email: xxbingliu@126.com

1. Introduction

The design and construction of coordination polymers (CPs) have attracted much attention [1–5]. Many of these materials are suitable for uses in gas adsorption, luminescence, magnetism, ion exchange, etc. [6–15]. Many synthetic approaches have been used to construct desired CPs through assembly of various metal centers with elaborately designed organic spacers [16–20]. In this context, 1,3-di(4-carboxyl-phenyl)benzene as the carboxylate ligand was used based on the following reasons: (a) the two carboxylate groups can adopt different types of coordination modes; (b) the benzene ring containing carboxylate groups can rotate around the central benzene ring that may lead to zigzag or helical chains. Isomeric N-donor ligands are also applied to study the effects of the organic linkers, of great importance in understanding the relationship between structures and intrinsic properties [21, 22].

Zn(II) complexes have interest due to appealing structures and photoluminescent properties. We used 1,3-di(4-carboxyl-phenyl)benzene and isomeric N-donor ligands to construct two Zn(II) CPs, $\{[Zn(dpb)(3\text{-}bpmp)_{0.5}]\cdot 1.5(DMF)\}_n$ (**1**) and $[Zn(dpb)(4\text{-}bpmp)]_n$ (**2**). The complexes display different topological nets. Luminescent properties for **1** and **2** were investigated.

2. Experimental

2.1. *General material and method*

All reagents and solvents were commercially available and used as received. Elemental analyses (C, H, and N) were performed with a VarioEL III Elemental analyzer. Infrared spectra of KBr pellets were recorded with a BRUKER EQUINOX-55 spectrometer from 4000 to 400 cm^{-1}. X-ray powder diffraction (XRPD) measurements were performed on a Bruker D8 diffractometer operated at 40 kV and 40 mA using Cu-Kα radiation ($\lambda = 0.15418$ nm). Luminescence spectra for solid samples were recorded with a Hitachi F-4500 fluorescence spectrophotometer at room temperature. Topological analyses were performed and confirmed by the Topos program [23, 24].

2.2. *Syntheses*

2.2.1. Preparation of $\{[Zn(dpb)(3\text{-}bpmp)_{0.5}]\cdot 1.5(DMF)\}_n$ (1). A mixture of $Zn(NO_3)_2\cdot 6H_2O$ (0.149 g, 0.5 mM), H_2dpb (0.159, 0.5 mM), 3-bpmp (0.240 g, 1 mM), and DMF (10 mL) was added to a 25 mL vial. The vial was sealed, held at 120 °C for 4 days, and then cooled to room temperature. Colorless crystals of **1** were obtained in 76% yield based on Zn. Anal. Calcd (%) for $C_{67}H_{65}Zn_2N_5O_{11}$: C, 64.53; H, 5.25; N, 5.62. Found: C, 64.52; H, 5.25; N, 5.63. IR (KBr pellet)/cm^{-1}: 3156w, 2863w, 1631s, 1521m, 1336m, 1137m, 1097m, 956m, 859m, 753m.

2.2.2. Preparation of $[Zn(dpb)(4\text{-}bpmp)]_n$ (2). Colorless crystals of **2** were obtained in 68% yield based on Zn by a procedure similar to that used for **1** except DMF was replaced by NMF (NMF = N-methyl formamide). Anal. Calcd (%) for $C_{36}H_{32}ZnN_4O_4$: C, 66.52; H, 4.96; N, 8.62. Found: C, 66.54; H, 4.95; N, 8.63. IR (KBr pellet)/cm^{-1}: 1605s, 1533m, 1397m, 1103m, 1033m, 993m, 837m, 797m.

Table 1. Crystallographic data and details of diffraction experiments for **1** and **2**.

	1	**2**
Formula	$C_{67}H_{65}Zn_2N_5O_{11}$	$C_{36}H_{32}ZnN_4O_4$
M_r	1246.98	650.03
Crystal system	Monoclinic	Monoclinic
Space group	*C2/c*	*C2/c*
a (Å)	28.566(5)	14.190(5)
b (Å)	9.2640(16)	23.941(5)
c (Å)	26.188(5)	20.597(5)
β (°)	117.254(3)	106.268(5)
V (Å^3)	6160.9(19)	6717(3)
Z	4	8
F(0 0 0)	2600	2704
Limiting indices	$-36 \le h \le 29$ $-12 \le k \le 10$ $-33 \le l \le 33$	$-18 \le h \le 18$ $-22 \le k \le 30$ $-26 \le l \le 26$
R_{int}	0.025	0.023
Absorption coefficient	0.843	0.774
Data/restraints/parameters	6993/7/390	7585/0/418
ρ (g cm^{-3})	1.344	1.286
R_{int}	0.025	0.023
$R_1{}^a$, $wR_2{}^b$ [$I > 2\sigma(I)$]	$R_1 = 0.0576$ $wR_2 = 0.1963$	$R_1 = 0.0437$ $wR_2 = 0.1277$
$R_1{}^a$, $wR_2{}^b$ (all data)	$R_1 = 0.0656$ $wR_2 = 0.2051$	$R_1 = 0.0562$ $wR_2 = 0.1335$
Gof	0.970	1.115
Max/min (e Å^{-3})	1.213/−0.619	0.865/−0.375

$^a R = \Sigma(||F_o| - |F_c||)/\Sigma|F_o|$. $^b wR = [\Sigma w(|F_o|^2 - |F_c|^2)^2/\Sigma w(F_o{}^2)]^{1/2}$.

Table 2. Selected bond lengths (Å) and angles (°) for **1** and **2**.

1			
Zn1–O2^{i}	2.025(3)	Zn1–O3^{iii}	2.048(3)
Zn1–N1	2.028(3)	Zn1–O1	2.049(3)
Zn1–O4^{ii}	2.041(2)	O4^{ii}–Zn1–O3^{iii}	159.48(12)
O2^{i}–Zn1–N1	106.44(13)	O2^{i}–Zn1–O1	159.12(14)
O2^{i}–Zn1–O4^{ii}	87.64(13)	N1–Zn1–O1	94.41(13)
N1–Zn1–O4^{ii}	101.13(12)	O4^{ii}–Zn1–O1	87.44(13)
O2^{i}–Zn1–O3^{iii}	88.82(13)	O3^{iii}–Zn1–O1	88.72(13)
N1–Zn1–O3^{iii}	99.26(12)		
2			
Zn1–N1	2.0543(18)	Zn1–O1	2.002(4)
Zn1–N1a^{i}	2.0543(18)	Zn1–O1a^{i}	2.002(4)
N1^{i}–Zn1–N1	103.03(10)	O1–Zn1–N1	103.98(14)
O1–Zn1–O1Aa^{i}	153.6(3)	O1–Zn1–N1a^{i}	92.47(13)
O1a^{i}–Zn1–N1a^{i}	103.98(14)	O1a^{i}–Zn1–N1	92.47(13)

Symmetry codes: For **1** (i) $-x + 3/2, -y + 5/2, -z + 2$; (ii) $-x + 1, y + 1, -z + 3/2$; (iii) $x + 1/2, -y + 3/2, z + 1/2$; For **2** (i) $-x + 1, y, -z + 1/2$.

2.3. *X-ray data collection and structure determinations*

Single crystals of **1** and **2** were prepared. X-ray crystallographic data of **1** and **2** were collected at room temperature using epoxy-coated crystals mounted on a glass fiber. All measurements were made on a Bruker SMART APEX II CCD diffractometer equipped with graphite monochromated Mo-Kα radiation ($\lambda = 0.71073$ Å) by using a ω-scan mode.

Empirical absorption correction was applied using SADABS [25]. All structures were solved by direct methods and refined by full-matrix least-squares on F^2 using SHEXL 97 [26]. All non-hydrogen atoms were refined anisotropically. The hydrogens were located by geometric calculations, and their positions and thermal parameters were fixed during the structure refinement. The crystallographic data and experimental details of structural analyses for **1** and **2** are summarized in table 1. Selected bond and angle parameters are listed in table 2.

3. Results and discussion

3.1. *Description of the crystal structures*

3.1.1. $\{[Zn(dpb)(3\text{-}bpmp)_{0.5}]\cdot 1.5(DMF)\}_n$ (1). The unit for $\{[Zn(dpb)(3\text{-}bpmp)_{0.5}]\cdot 1.5(DMF)\}_n$ (**1**) is shown in figure 1. There is one crystallographically independent Zn(II), one dpd, and a half of 3-bpmp in the asymmetric unit. Zn(II) is a five coordinate with four oxygens from four dpb ligands [Zn–O, ranging from 2.025(3) to 2.048(3) Å] and one nitrogen from 3-bpmp [Zn(1)–N(1) = 2.028(3) Å] to give a square pyramidal geometry. The equatorial plane is defined by O1, O2, O3, and O4 (the equation of plane is $0.5654x - 0.7447y - 0.3547z = 0.5227$ with the maximal and the mean deviation being 0.0029 and 0.0022 Å, respectively). Two Zn(II) ions, related by a twofold axis, are bridged by two pairs of carboxylate ligands to form a dinuclear Zn(II) unit with Zn···Zn distance of 2.953 Å. The $[Zn(CO_2)_4Zn]$ dimers are bonded to four dpb^{2-} ligands. The dimers, thus, can be viewed as a 4-connected node to generate a two-dimensional (2-D) layer that forms a series of layered

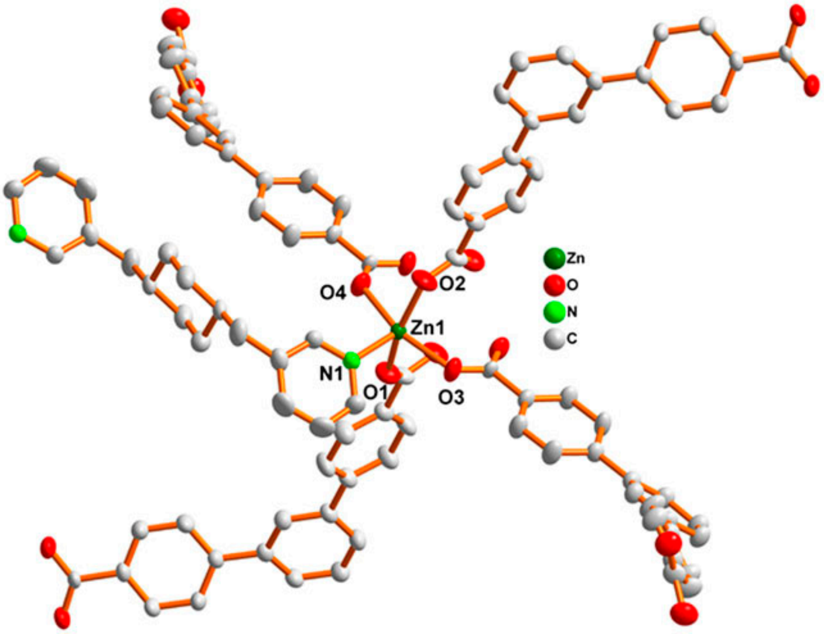

Figure 1. The coordination environment of the Zn(II) ion in **1**.

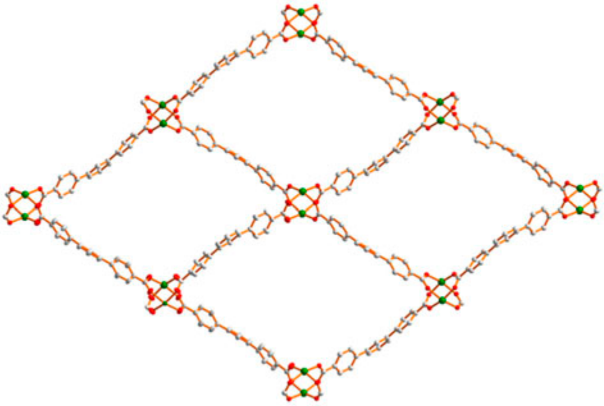

Figure 2. The 2-D layer constructed by carboxylate ligands and Zn(II) ions.

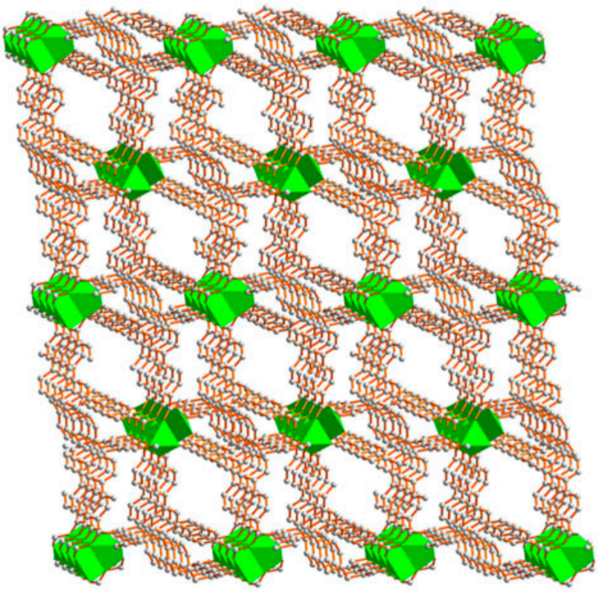

Figure 3. The 3-D structure for **1**.

squares (figure 2). The sheets are then bridged by 3-bpmp ligands to generate a three-dimensional (3-D) structure (figure 3). Each [Zn(CO_2)$_4$Zn] dimer is bridged to structural units in the sheet above and below by pairs of 3-bpmp ligands. From a topological view, the [Zn(CO_2)$_4$Zn] unit can be treated as a six-connected node, the organic ligands can be regarded as linkers, and the 3-D structure can be simplified as a 6-connected topological net with point symbol ($4^4.6^{11}$) (figure 4).

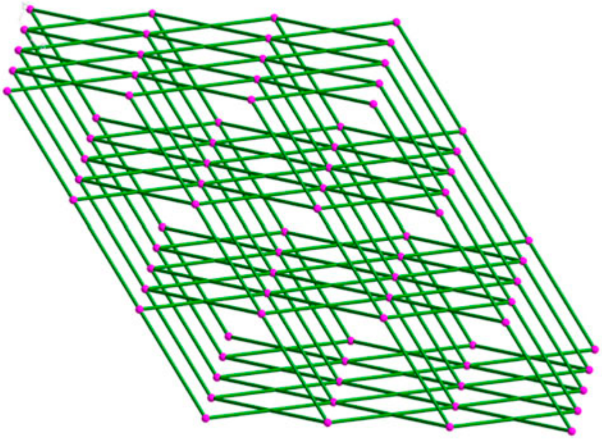

Figure 4. The 6-connected topological net for **1** with point symbol ($4^4.6^{11}$).

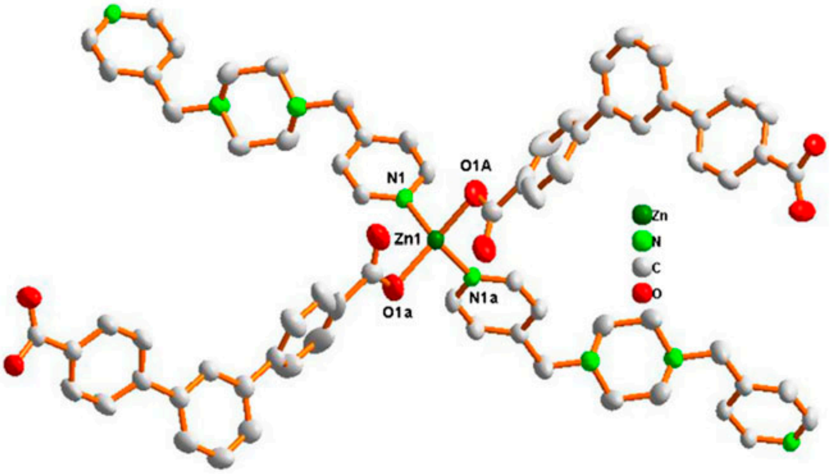

Figure 5. The coordination environment of the Zn(II) ion in **2**.

3.1.2. [Zn(dpb)(4-bpmp)]$_n$ (2). Single-crystal X-ray diffraction analysis reveals that **2** crystallizes in the monoclinic space group *C2/c* and exhibits an interesting three-fold interpenetrated 3-D framework. In the asymmetric unit of **2**, there is one Zn(II), one dpd^{2-}, and one 4-bpmp. As shown in figure 5, the Zn(II) exhibits a four-coordinate environment with two carboxylate oxygens [Zn(1)–O(1) = 2.002(4) Å] and two nitrogens [Zn(1)–N(1) = 2.0543(18) Å]. In **2**, the 4-bpmp ligands connect Zn(II) to form one-dimensional (1-D) zigzag chains (figure S1, see online supplemental material at http://dx.doi.org/10.1080/00958972.2015.1019484). The carboxylates link Zn(II) to construct a 1-D helical chain with pitch of 28.38 Å [figure 6(a) and (b)]. In **2**, the 1-D zigzag chains and 1-D helical chains are interwoven to form a 3-D structure [figure 6(c)]. Based on topological theory, the Zn(II) ions and organic linker can be regarded as nodes and linkers, and the 3-D structure

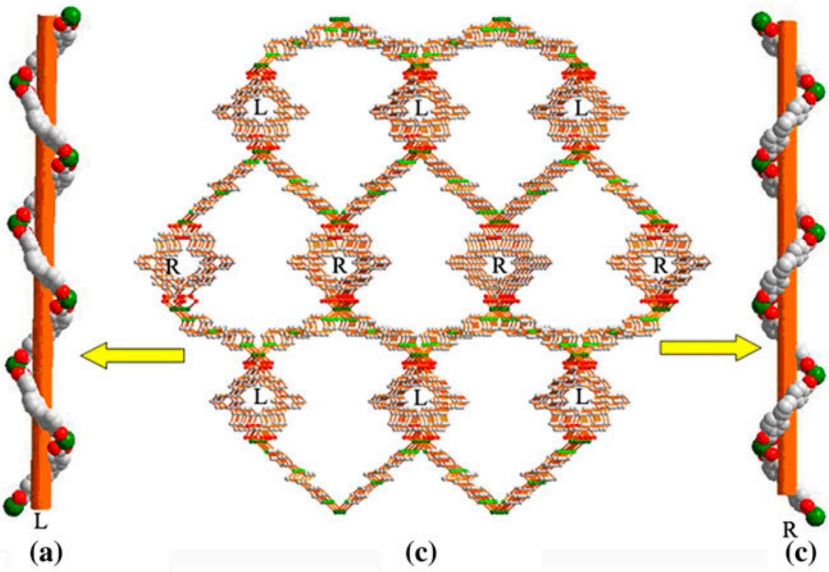

Figure 6. (a) Left-handed helical chain; (b) right-handed helical chain; and (c) the 3-D structure for **2**.

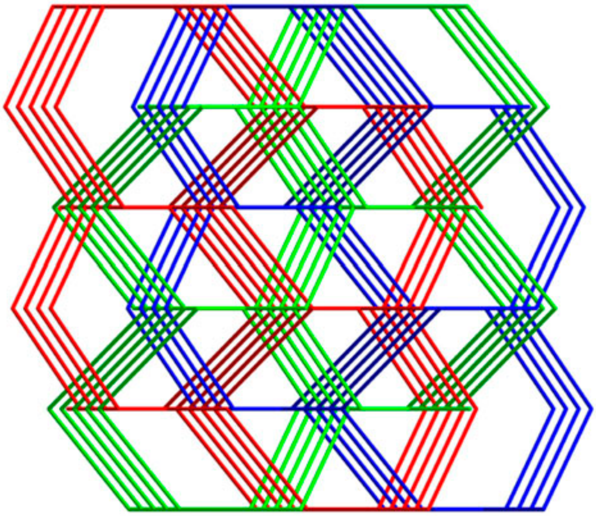

Figure 7. The 4-connected three-fold interpenetrated topology for **2**.

can be simplified as a 6-connected topological net with point symbol (6^5.8). The void space in an individual framework is sufficiently large that three identical 3-D frameworks interpenetrate with each other to form an intriguing three-fold interpenetrated structure (figure 7). The interpenetration vectors are [1/2, 1/2, 0] and [1/2, −1/2, 0] (13.92 Å).

Complexes **1** and **2** are both six-connected nets and possess different topologies. Related Zn(II) CPs are cited as structural comparisons. Thus, Gao and coworkers reported [Zn(bimb) (bdc)]·H_2O and [Zn(bimb)(Hbtc)]·H_2O [bimb = 4,4′-bis(1H-imidazol-1-yl-methyl)biphenyl; H_2bdc = 1,2-benzenedicarboxylic acid; H_3btc = 1,3,5-benzenetricarboxylic acid], showing a 3-D uoc type topology with two-fold interpenetration and a 2-D self-penetrating network via hydrogen bonds, respectively [27]. Zhang and coworkers obtained {[Zn(IIP)(bbtz)(H_2O)]·H_2O}$_n$ and [Zn(IIP)(bbtz)] based on 5-iodoisophthalic acid (IIP) and 1,4-bis(triazol-1-ylmethyl)benzene (bbtz), displaying the 3-D supramolecular structures via the $\pi\cdots\pi$ stacking interactions, hydrogen bonds, and C–I···O halogen bonds, respectively [28]. Meng and coworkers synthesized {[Zn(imb)(SO4)]·H_2O}$_n$ (imb = 2-(1H-imidazol-methyl)-1Hbenzimidazole), which features a 2-D (4,4) network and further extends to a 3-D supramolecular structure by hydrogen bonding interactions [29]. Li and coworkers obtained three Zn(II) CPs, [Zn(DMTDC)(bpt)(H_2O)]$_n$, {[Zn(DMTDC)(5,5′dimbpy)]·0.5DMF·1.5H_2O}$_n$, and {[Zn(DMTDC)(1,3-bimb)]·2DMF·H_2O}$_n$ (H_2DMTDC = 3,4dimethythieno(2,3-b)thiophene-2,5-dicarboxylic acid, bpt = 4-amino-3,5-bis(4-pyridyl)1,2,4triazole, 5,5′-dimbpy = 5,5′-dimethyl-2,2′-bipyridyl, 1,3-bimb = 1,3-bis(imdazol-1-ylmethyl)benzene). [Zn(DMTDC)(bpt)(H_2O)]$_n$ and {[Zn(DMTDC)(5,5′dimbpy)]·0.5DMF·1.5H_2O}$_n$ display the 1-D linear and zigzag chain with different supramolecular structures. {[Zn(DMTDC)(1,3-bimb)]·2DMF·H_2O}$_n$ features 3-D polycatenations [30]. Fang and coworkers reported {[Zn(H_2BPDC)(SO_4)]}$_n$ (BPDC = 2,2′-bipyridine-5,5′-dicarboxylic anion) which displays a 3-D structure [31].

3.2. *Luminescent properties*

XRPD was performed to check the phase purities of the complexes. As shown in figure S1 (supporting information), peak positions of the simulated and experimental XRPD patterns are in agreement with each other, demonstrating single-phase purity of products. The difference in intensity may be due to the preferred orientation of the microcrystalline powder samples.

The luminescent emission spectra of **1** and **2** are shown in figure 8. Intense photoluminescence emissions for **1** and **2** are observed at 503 nm (λ_{ex} = 307 nm) and 515 nm (λ_{ex} = 323 nm), respectively. The 3-bpmp and 4-bpmp exhibit broad weak fluorescent emissions centered at 545 nm (λ_{ex} = 277 nm) and 524 nm (λ_{ex} = 330 nm), respectively [32].

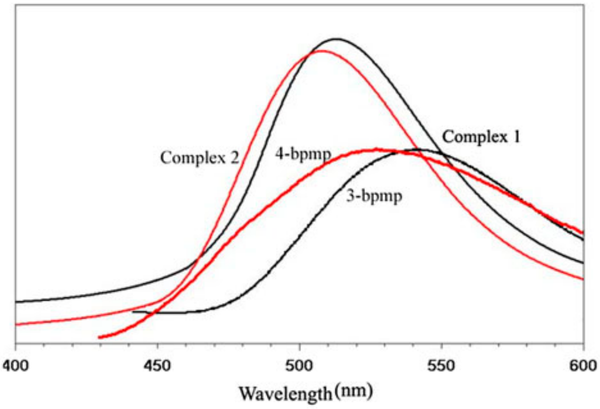

Figure 8. Solid-state luminescent emission spectra for **1** and **2** at room temperature.

The emissions for **1** and **2** are tentatively assigned to ligand-localized luminescence considering their emission features are similar to that of the free ligand. Zn(II) is difficult to oxidize or reduce owing to the d^{10} configuration. The enhancement of the intensity in the metal complex may be attributed to increased rigidity of the ligand upon metal coordination, which effectively reduces energy loss [33, 34].

4. Conclusion

We use dicarboxylate and N-donor coligands to construct two Zn(II) CPs. The results indicate that isomeric N-donor ligands can affect final structures of the CPs. Furthermore, the luminescent properties of **1** and **2** were investigated.

Supplementary material

Crystallographic data have been deposited at the Cambridge Crystallographic Data Center as supplementary publications (CCDC: 1019748 and 1019749). The data can be obtained free of charge via http://www.ccdc.cam.ac.uk/conts/retrieving.html, or from the Cambridge Crystallographic Data Center, 12 Union Road, Cambridge CB2 1EZ, UK; Fax: (+44)1223 336 033; or E-mail: deposit@ccdc.cam.ac.uk.

References

[1] J. Fan, M.H. Shu, T.A. Okamura, Y.Z. Li, W.Y. Sun, W.X. Tang, N. Ueyama. *New J. Chem.*, **27**, 1307 (2003).
[2] G.X. Liu, K. Zhu, H. Chen, R.Y. Huang, H. Xu, X.M. Ren. *Inorg. Chim. Acta*, **362**, 1605 (2009).
[3] Y.Y. Lin, Y.B. Zhang, J.P. Zhang, X.M. Chen. *Cryst. Growth Des.*, **8**, 3673 (2008).
[4] W. Wang, P. Xi, X. Su, J. Lan, Z. Mao, J. You, R. Xie. *Cryst. Growth Des.*, **7**, 741 (2007).
[5] K. Ma, J. You. *Chem. Eur. J.*, **13**, 1863 (2007).
[6] Y.L. Liu, J.F. Eubank, A.J. Cairns, J. Eckert, V.Ch. Kravtsov, R. Luebke, M. Eddaoudi. *Angew. Chem. Int. Ed.*, **46**, 3278 (2007).
[7] Y.B. Zhang, W.X. Zhang, F.Y. Feng, J.P. Zhang, X.M. Chen. *Angew. Chem. Int. Ed.*, **48**, 5287 (2009).
[8] Z.M. Man, F. Guo. *J. Coord. Chem.*, **66**, 1 (2013).
[9] D.S. Deng, P. Liu, W.J. Fu, L. Li, F.X. Yang, B.M. Ji. *Inorg. Chim. Acta*, **363**, 891 (2013).
[10] R. Cao, Q. Shi, D.F. Sun, M.C. Hong, W.H. Bi, Y.J. Zhao. *Inorg. Chem.*, **41**, 6161 (2002).
[11] K.S. Gavrilenko, S.V. Punin, O. Cador, S. Golhen, L. Ouahab, V.V. Pavlishchuk. *J. Am. Chem. Soc.*, **127**, 12246 (2005).
[12] Y. Wang, P. Cheng, Y. Song, D.Z. Liao, S.P. Yan. *Chem. Eur. J.*, **13**, 8131 (2007).
[13] L.H. Xie, S.X. Liu, C.Y. Gao, R.G. Cao, J.F. Cao, C.Y. Sun, Z.M. Su. *Inorg. Chem.*, **46**, 7782 (2007).
[14] J. Wu, H.W. Hou, Y.X. Guo, Y.T. Fan, X. Wang. *Eur. J. Inorg. Chem.*, **2009**, 2796 (2009).
[15] Y. Ji, R. Zhang, Y.J. Li, Y.Z. Li, J.L. Zuo, X.Z. You. *Inorg. Chem.*, **46**, 866 (2007).
[16] L. Chen, G.J. Xu, K.Z. Shao, Y.H. Zhao, G.S. Yang, Y.Q. Lan, X.L. Wang, H.B. Xu, Z.M. Su. *CrystEngComm*, **12**, 2157 (2010).
[17] Y. Liu, N. Li, L. Li, H.L. Guo, X.F. Wang, Z.X. Li. *CrystEngComm*, **14**, 2080 (2012).
[18] Y. Liu, Y. Qi, Y.H. Su, F.H. Zhao, Y.X. Che, J.M. Zheng. *CrystEngComm*, **12**, 3283 (2010).
[19] N. Chen, J. Zhang, Y.C. Gao, Z.L. Yang, H.J. Lu, G. Li. *J. Coord. Chem.*, **64**, 2554 (2011).
[20] K. Yang, Z.Z. Wang, Z.H. Liu. *J. Coord. Chem.*, **63**, 2286 (2010).
[21] F. Guo, F. Wang, H. Yang, X.L. Zhang, J. Zhang. *Inorg. Chem.*, **51**, 9677 (2012).
[22] L. Zhao, F. Guo. *Z. Anorg. Allg. Chem.*, **640**, 168 (2014).
[23] V.A. Blatov. *IUCr CompComm Newsletter*, **7**, 4 (2006).
[24] V.A. Blatov, A.P. Shevchenko, V.N. Serezhkin. *J. Appl. Crystallogr.*, **33**, 1193 (2000).
[25] *SAINT Software Reference Manual*, Bruker AXS, Madison, WI (1998).
[26] G.M. Sheldrick, *SHELXTL NT, Version 5.1, Program for Solution and Refinement of Crystal Structures*, University of Göttingen, Göttingen (1997).

[27] Y.H. Yu, B. Wen, H.Z. Zhang, G.F. Hou, J.S. Gao, P.F. Yan. *J. Coord. Chem.*, **67**, 588 (2014).
[28] K.L. Zhang, C.Y. Jing, Y. Deng, L. Zhang, Q.H. Meng, P.Z. Zhu, S.W. Ng. *J. Coord. Chem.*, **67**, 1596 (2014).
[29] W.L. Duan, Y.H. Zhang, X.X. Wang, X.R. Meng. *J. Coord. Chem.*, **67**, 1980 (2014).
[30] T.T. Cao, J. Lu, S.N. Wang, C.H. Zhou, J.M. Dou, D.C. Li, D.Q. Wang. *J. Coord. Chem.*, **67**, 1948 (2014).
[31] M. Fang, T. Wang, X.L. Lu, A.J. Song, L. Shen, H.Y. Tian. *J. Coord. Chem.*, **67**, 2280 (2014).
[32] K.K. Bisht, E. Suresh. *Cryst. Growth Des.*, **13**, 664 (2013).
[33] L.L. Wen, D.B. Dang, C.Y. Duan, Y.Z. Li, Z.F. Tian, Q.J. Meng. *Inorg. Chem.*, **44**, 7161 (2005).
[34] T.L. Hu, R.Q. Zou, J.R. Li, X.H. Bu. *Dalton Trans.*, **2008**, 1302 (2008).